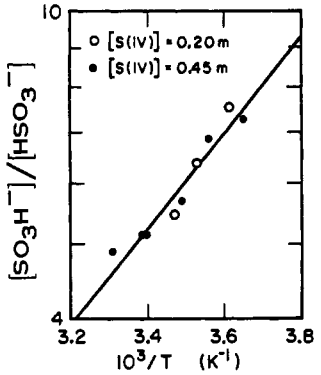

Figure 2. Temperature dependence of the equilibrium quotient Q_2 for the reaction $HSO_3^- = SO_3H^-$. The equilibrium quotient was determined at an ionic strength of 1.0 *m* for solutions having S(IV) concentrations of 0.20 and 0.45 *m*. The straight line represents the nonweighted linear-least-squares fit of the data and has the equation $\ln Q_2 = (-3.232 \pm 0.5274) + (1438 \pm 151.2)/T$, with a covariance of -79.71 between the slope and *y* intercept.

SO_3^{2-}, and $S_2O_5^{2-}$ were calculated for the pH 5 solutions, and the fraction of the 193 ppm peak area attributable to bisulfite ion was determined. The area corresponding to the total bisulfite ion concentration in the pH 3 solution was obtained by multiplying the area corresponding to the total bisulfite ion concentration in the pH 5 solution by the ratio of the calculated bisulfite ion concentration at pH 3 to that calculated at pH 5. To minimize error arising from the estimated value of the equilibrium quotient for the dimerization of bisulfite ion (which was used in calculating the bisulfite ion concentrations), a pH 5 solution having nearly the same bisulfite concentration as the pH 3 solution was always used.

The values of the parameters used in the calculation of Q_2 are listed in Table II together with the resulting values of the equilibrium quotient. Figure 2 shows a plot of log Q_2 vs. $1/T$. A nonweighted linear-least-squares treatment of the data yields

$$\ln Q_2 = (-3.232 \pm 0.5274) + (1438 \pm 151.2)/T \quad (5)$$

as the equation of the best straight line through the points, with a covariance of -79.71 between the slope and *y* intercept. From the values of the slope and intercept one obtains $\Delta H_2 = -2.9 \pm 0.3$ kcal/mol and $\Delta S_2 = -6 \pm 1$ cal K^{-1} mol^{-1}.

The oxygen-17 NMR spectra of bisulfite solutions provide the most convincing evidence to date for the existence of the two isomers of bisulfite ion, HSO_3^- and SO_3H^-, and allow the first measurement of their equilibrium concentration ratio.

Acknowledgment. This work was supported by the Director, Office of Energy Research, Office of Basic Energy Sciences, Chemical Science Division of the U.S. Department of Energy, under Contract No. DE-AC03-76SF00098.

Registry No. HSO_3^-, 15181-46-1; O_2, 7782-44-7.

Contribution from the Department of Chemistry and the Department of Biochemistry and Biophysics, University of Pennsylvania, Philadelphia, Pennsylvania 19104

Divalent Metal Ion Binding Sites on Yeast Inorganic Pyrophosphatase As Studied by CW-EPR and Electron Spin Echo Measurements on the Copper(II) Enzyme

Amit Banerjee,† Russell LoBrutto,‡ and Barry S. Cooperman*†

Received November 4, 1985

Cu(II) EPR is used to probe the divalent metal ion binding sites of yeast inorganic pyrophosphatase (PPase). Measurements of *g* and *A* values for the highest affinity site provide clear evidence for exclusive oxygen coordination to Cu(II) in a distorted octahedral environment. The absence of electron spin echo envelope modulation provides evidence against histidine side-chain binding to Cu(II). Examination of the CW-EPR spectrum along with measurement of spin-lattice relaxation times (T_1) of enzyme-bound Cu(II), as functions of Cu(II):PPase stoichiometry in both the absence and the presence of either inorganic phosphate or hydroxymethylenediphosphonate, allows formulation of a three-site model for Cu(II) binding to PPase. In this model the strongest interaction is between the two Cu(II) ions bound per subunit in the absence of a phosphoryl ligand, and there is some interaction between one of these sites and the third Cu(II) site that accompanies the binding of a phosphoryl ligand. Evidence that the Cu(II) sites observed are relevant for the active site of PPase is provided by the observation that Cu(II) serves as a divalent metal ion cofactor for enzymatic activity (although it confers only 0.1% of the activity found with Mg^{2+}), by the sensitivity of both CW-EPR and T_1 measurements to added phosphoryl ligands, and by the strong competition by Mg^{2+} for at least one of the three Cu(II) sites.

Introduction

Yeast inorganic pyrophosphatase (PPase) (E.C. 3.6.1.1) is a metal ion activated enzyme, catalyzing both hydrolysis of pyrophosphate (PPi) and oxygen exchange between water and orthophosphate (Pi).[1] PPase consists of two identical subunits of molecular weight 32 000.[2,3] Rapoport et al.[4] have shown that native PPase binds two divalent metal ions (Mg(II), Co(II), Mn(II), or Zn(II)) per enzyme subunit. Recent studies by ourselves and others have shown that in the presence of either PPi or Pi the enzyme binds a third and even a fourth divalent metal ion per subunit and, in addition, that three divalent metal ions per subunit are required for activity.[5-8] Two important questions are raised by these results: First, what are the structures of the metal ion binding sites on the enzyme? Second, what is the nature of metal ion-metal ion interaction on the enzyme surface?

In previous studies we have employed ^{113}Cd NMR[9] and Mn(II) EPR[10] to obtain at least partial answers to these questions. In the present work we continue our investigation through use of

* To whom correspondence should be addressed.
† Department of Chemistry.
‡ Department of Biochemistry and Biophysics.

(1) Cooperman, B. S. *Methods Enzymol.* **1982**, *87*, 526.
(2) Heinrikson, R. L.; Sterner, R.; Noyes, C.; Cooperman, B. S.; Bruckmann, R. H. *J. Biol. Chem.* **1973**, *248*, 2521.
(3) Cohen, S. A.; Sterner, R.; Keim, P. S.; Heinrikson, R. L. *J. Biol. Chem.* **1978**, *253*, 889.
(4) Rapoport, T. A.; Hohne, W. E.; Heitmann, P.; Rapoport, S. *Eur. J. Biochem.* **1973**, *33*, 341.
(5) Cooperman, B. S.; Panackal, A.; Springs, B.; Hamm, D. J. *Biochemistry* **1981**, *20*, 6051.
(6) Springs, B.; Welsh, K. M.; Cooperman, B. S. *Biochemistry* **1981**, *20*, 6384.
(7) Welsh, K. M.; Armitage, I. M.; Cooperman, B. S. *Biochemistry* **1983**, *22*, 1046.
(8) Knight, W. B.; Dunaway-Mariano, D.; Ransom, S. C.; Villafranca, J. J. *J. Biol. Chem.* **1984**, *259*, 2886.
(9) Welsh, K. M.; Cooperman, B. S. *Biochemistry* **1984**, *23*, 4947.
(10) Banerjee, A.; Cooperman, B. S. *Inorg. Chim. Acta* **1983**, *79* (B7) 146.

0020-1669/86/1325-2417$01.50/0

Cu(II) EPR. Cu(II) complexes are usually distorted octahedra or, in the limiting case, square planar.[11] The EPR spectra of distorted octahedral complexes typically show a higher intensity absorption at higher field, characterized by spectral parameters $g_\perp$ and $A_\perp$, and a lower intensity absorption at lower field, characterized by spectral parameters $g_\parallel$ and $A_\parallel$, and it has been demonstrated that these parameters can be used to identify the coordination geometry and coordinating ligand atoms in Cu(II) complexes.[12] In this paper we measure g and A values for Cu(II) bound to PPase in the presence and absence of Pi and of the competitive inhibitor hydroxymethylenediphosphonate (PCHOHP).[13] These measurements, along with measurements of the CW-EPR spectral line widths and spin–lattice relaxation times (T_1) of enzyme-bound Cu(II), have (a) provided clear indications of the structure of at least one Cu(II) binding site on PPase, (b) revealed clear differences in the binding of Cu(II) in the presence and absence of phosphoryl ligands, (c) provided estimates for Cu(II)–Cu(II) interaction on the enzyme surface, and (d) allowed formulation of a three-site model for Cu(II) binding to PPase.

Experimental Procedures

Materials. PPase, prepared as described previously[14] with modifications,[15] was >94% homogeneous as judged by SDS polyacrylamide-gel electrophoresis, and ranged in specific activity from 480 to 720 μmol of PPi hydrolyzed min^{-1} mg^{-1} as determined by the standard titrimetric assay.[14] Protein could be regenerated free of divalent metal ion by equilibration against Chelex-100 (Na^+ form) in 50 mM Tris·HCl (pH 7.0), followed by removal of the resin. The enzyme was routinely concentrated under nitrogen with an Amicon stir cell containing a PM-10 filter. The protein concentration was determined by A_{280}, with use of an extinction coefficient for a 0.1% solution equal to 1.45.[16] A subunit molecular weight of 35 kilodaltons was assumed in these calculations.[17] Cu(II) solutions were standardized at atomic absorption spectroscopy with an AAS standard solution (Alfa Products). The PCHOHP was a gift of Dr. D. A. Nichols of Proctor and Gamble. $H_2{}^{17}O$ (13% ^{16}O, 52% ^{17}O, and 35% ^{18}O) was purchased from Monsanto. All other chemicals were reagent grade and were used without further purification.

^{17}O-Enriched PCHOHP. The procedure described by Gerlt et al.[18] for the preparation of ^{17}O-enriched methylenediphosphonic acid was followed. This method yielded 15% enriched ^{17}O in each of the phosphoryl oxygens, as determined by mass spectral analysis with a Hitachi Perkin-Elmer RMH-2 spectrometer.

EPR Experiments. A Varian E-109 spectrometer with a variable-temperature unit was used to record EPR spectra at the X-band. All titrations were carried out by adding aliquots of 0.05 M $CuCl_2$ to PPase in 0.1 M Tris·HCl, 0.1 M KCl buffer, pH 7.2 (Buffer A), in the presence or absence of PCHOHP. In the absence of enzyme, the EPR spectrum of Cu(II) in buffer A was isotropic, and showed no $g_\parallel$ absorption. EPR spectra were taken on an enzyme solution aliquot after each addition of Cu(II). The aliquot was subsequently returned to the mixing tube and the titrations continued. Liquid-state spectra at −6 °C were recorded in a quartz tube of inner diameter 0.5 mm; for frozen samples, quartz tubes of inner diameter 3 mm (samples containing either PPase alone, or PPase plus PCHOHP) or 0.5 mm (samples containing PPase plus Pi) were used. The instrument settings were as follows: microwave frequency, 9.18 GHz; power, 20 mW; modulation amplitude, 1 mT; scan rate, 22.5 mT/min; time constant, 0.25 s. A spectral width of 100 mT, centered at 300 mT, was used unless otherwise stated.

T_1 Experiments. Measurements of electron spin–lattice relaxation times (T_1) were made on a pulsed EPR spectrometer, which employed a Varian E-4 magnet and a 40-W ITT traveling wave tube amplifier. The microwave circuitry is of coaxial construction except for a waveguide circulator. In order to compensate for the low Q-factor necessary in pulsed measurements, a "current sheet" microwave resonator was used in place of a resonant cavity.[19] This structure consists of two thin copper foil lobes mounted on a quartz tube and inserted in the inner bore of an Air Products liquid-helium flow cryostat. Coupling through the flow Dewar walls is accomplished with a small loop at the end of a length of semirigid coaxial cable, positioned near the bottom edge of one of the conducting lobes.

T_1 was measured by using a pulse sequence of the form: 180°–T–90°–τ–180°–τ–echo,[20] where τ was fixed at approximately 250 ns and T was varied smoothly between 0 and 500 μs. Echo amplitudes were measured by using an Evans Associates gated integrator module, the output of which was digitized by a Data Translation 2801 lab interface and stored in an IBM personal computer. Spin-echo decay curves were fitted to single exponentials by using the modified phase–plane method of Bacon and Demas.[21]

The titration procedure, employing a 3 mm inner diameter quartz sample tube, was essentially similar to that of the EPR experiment, except that rather than having aliquots removed, the enzyme solution (0.2 mL) was placed in the tube and aliquots of Cu(II) solution were added directly. PPase retained >95% of its activity after repeated freezing and thawing during these titrations.

ESEEM Measurements. Electron spin-echo envelope modulation (ESEEM) measurements employed a pulse sequence of the form 90°–τ–90°–T–90°–τ–echo, where τ was fixed in the 200–300-ns range and T was varied from 0 to 10 μs. As in the T_1 experiment, the length of a 90° pulse was about 80 ns.

PPase Activity. PPase activity was determined by measuring rates of ^{32}Pi formation on hydrolysis of ^{32}PPi.[6] Essentially identical results were obtained with either Fisher reagent grade $CuCl_2$ or Puratronic grade $CuCl_2$ solution (Johnson Matthey Chemicals, Ltd.).

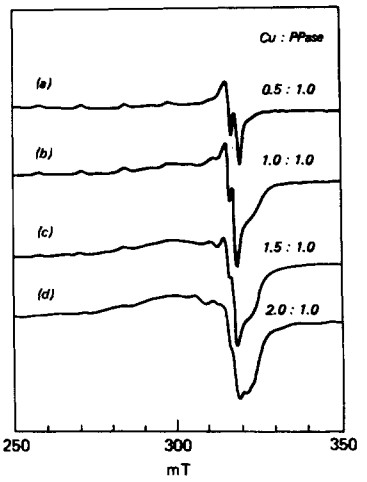

Figure 1. Liquid-state EPR spectra of solutions of PPase and varying Cu(II). Solutions had the following compositions: (a) 2.7 mM in PPase subunits, 1.35 mM in Cu(II); (b) 2.7 mM in both PPase subunits and Cu(II); (c) 2.7 mM in PPase subunits, 4.05 mM in Cu(II); (d) 2.7 mM in PPase subunits, 5.4 mM in Cu(II). Temperature = −6 °C. Receiver gain: (a) 3.2×10^3; (b–d) 2.5×10^3.

Results

Liquid-State EPR Spectra of Cu(II)–PPase in the Absence and Presence of Phosphoryl Ligands. EPR spectra were taken of solutions of Cu(II) and PPase as a function of the Cu(II):PPase stoichiometric ratio and in the absence and presence both of the competitive inhibitor PCHOHP and of Pi.

Spectra for solutions containing different Cu(II):PPase ratios are shown in Figure 1. The spectrum obtained at a ratio of 0.5 (Figure 1a) shows relatively sharp hyperfine structure, allowing evaluation of the $g_\parallel$, $g_\perp$, $A_\parallel$, and $A_\perp$ values collected in Table I. Hyperfine structure is retained and spectral intensity increases as the ratio is raised to 1.0 (Figure 1b), but a broad new shoulder centered at 322.5 mT is also visible. Finally, as the ratio is raised to 1.5 (Figure 1c) and then to 2.0 (Figure 1d), the spectrum broadens, the initial hyperfine structure is lost, and there is a clear decrease in the intensity of the $g_\perp$ peak. Close inspection of Figure 1c hints at the presence of an additional hyperfine structure, but

(11) Cotton, F. A.; Wilkinson, G. *Advanced Inorganic Chemistry*, 4th ed.; Wiley: New York, 1980; p 678.
(12) Peisach, J.; Blumberg, W. E. *Arch. Biochem. Biophys.* **1974**, *165*, 691.
(13) Cooperman, B. S.; Chiu, N. Y. *Biochemistry* **1973**, *12*, 1676.
(14) Cooperman, B. S.; Chiu, N. Y.; Bruckmann, R. H.; Bunick, G. J.; McKenna, G. P. *Biochemistry* **1973**, *12*, 1665.
(15) Bond, M. W. Ph.D. Thesis, University of Pennsylvania, Philadelphia, PA, 1979.
(16) Kunitz, M. *J. Gen. Physiol.* **1952**, *35*, 423.
(17) Bond, M. W.; Chiu, N. Y.; Cooperman, B. S. *Biochemistry* **1980**, *19*, 94.
(18) Gerlt, J. A.; Reynolds, M. A.; Demou, P. C.; Kenyon, G. L. *J. Am. Chem. Soc.* **1983**, *105*, 6469.
(19) LoBrutto, R.; Leigh, J. S., manuscript in preparation.
(20) Norris, J. R.; Thurnauer, M. C.; Bowman, M. K. *Adv. Biol. Med. Phys.* **1981**, *17*, 365.
(21) Bacon, J. R.; Demas, J. N. *Anal. Chem.* **1983**, *55*, 653.

Table I. CW-EPR Data for Cu(II)–PPase in the Presence and the Absence of Phosphoryl Ligands

sample compn	temp, °C	[PPase], mM	$g_\parallel$	$10^{-4}A_\parallel$, cm^{-1}	$g_\perp$	$10^{-4}A_\perp$, cm^{-1}	rel intens of $g_\perp$ line[a]
$Cu_{0.5}$PPase	−6	2.7	2.38	144	2.06	16	5.3
CuPPase	−6	2.7	2.38	148	2.06	16	10.4
$Cu_{1.5}$PPase	−6	2.7	2.38	148	2.06		9.9
Cu_2PPase	−6	2.7	...	...	2.06	...	9.0
$Cu_{0.5}$(PCHOHP)PPase	−6	2.7	2.38	144	2.06	15	3.0
Cu(PCHOHP)PPase	−6	2.7	2.38	144	2.06	15	6.4
$Cu_{1.5}$(PCHOHP)PPase	−6	2.7	2.38	148	2.06	15	11.4
			2.27	175	2.03	...	...
Cu_2(PCHOHP)PPase	−6	2.7	2.38	148	2.03	...	12.1
			2.27	175	...	...	...
Cu_3(PCHOHP)PPase	−6	2.7	...	...	2.03	...	...
$Cu_{0.5}(Pi)_{11}$PPase	−6.5	1.38	2.20	179	2.05	...	2.8
$Cu(Pi)_{11}$PPase	−6.5	1.38	2.20	179	2.05	...	8.1
$Cu_2(Pi)_{11}$PPase	−6.5	1.38	2.20	179	2.06	...	13.1
			2.36	150	...	...	
$Cu_3(Pi)_{11}$PPase	−6.5	1.38	2.20	180	2.06	...	14.7
$Cu_{0.5}$PPase	−94	0.2	2.27	205	2.03	15	6.8
CuPPase	−94	0.2	2.27	205	2.03	15	13.2
$Cu_{1.5}$PPase	−94	0.2	2.27	205	2.03	15	15.5
Cu_2PPase	−94	0.2	2.27	205	2.03	15	15.8
Cu(PCHOHP)PPase	−86	0.2	2.22	197	2.00	14	7.5
$Cu_{1.5}$(PCHOHP)PPase	−86	0.2	2.22	197	2.00	14	7.0
Cu_2(PCHOHP)PPase	−86	0.2	2.22	197	2.00	14	8.7
$Cu_{2.8}$(PCHOHP)PPase	−86	0.2	2.22	197	2.00	14	10.4
$Cu_{0.5}(Pi)_5$PPase	−37	2.5	2.26	185	2.02	12	6.1
$Cu_1(Pi)_5$PPase	−37	2.5	2.26	185	2.02	12	11.1
$Cu_2(Pi)_5$PPase	−37	2.5	2.26	185	2.02		11.3
$Cu_3(Pi)_5$PPase	−37	2.5	2.26	185	2.02		10.9

[a] Relative intensities are normalized on the basis of the lowest receiver gain for each set of titrations.

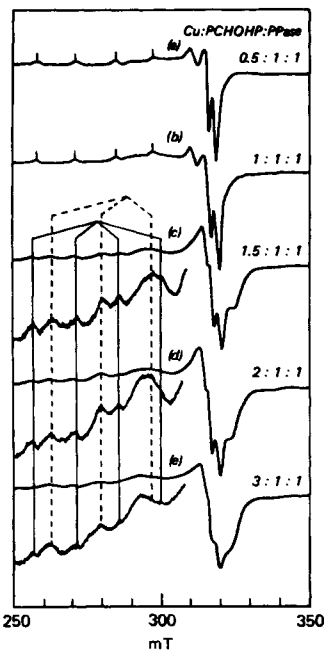

Figure 2. Liquid-state EPR spectra of solutions of PPase, PCHOHP, and varying Cu(II). All solutions were 2.7 mM in PPase subunits and PCHOHP and contained in addition (a) 1.35 mM Cu(II), (b) 2.7 mM Cu(II), (c) 4.05 mM, Cu(II), (d) 5.4 mM Cu(II), or (e) 8.1 mM Cu(II). Temperature = −6 °C. Receiver gain: (a) 3.2×10^3; (b–e) 1.6×10^3. For spectra c–e, the $g_\parallel$ region was also recorded at a receiver gain of 8×10^3, as shown.

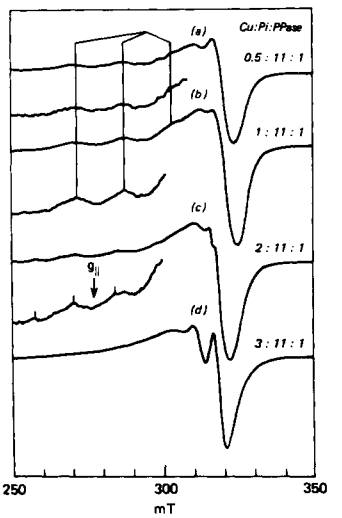

Figure 3. Liquid-state EPR spectra of solutions of PPase, Pi, and varying Cu(II). All solutions were 1.38 mM in PPase subunits and 15.2 mM in Pi and contained in addition (a) 0.7 mM Cu(II), (b) 1.38 mM Cu(II), (c) 2.76 mM Cu(II), or (d) 4.14 mM Cu(II). Temperature = −6.5 °C. Receiver gain: (a–c) 2.5×10^3; (d) 1.6×10^3. For spectra a–c, the $g_\parallel$ region was also recorded at a receiver gain of 10×10^3, as shown.

the broad nature of these peaks prevented a reliable measure of a $g_\parallel$ value.

Repetition of the Cu(II) titration of PPase but in the presence of PCHOHP (Figure 2) leads to some interesting similarities and differences. Up until a ratio of 1.0 (Figure 2a,b) the addition of PCHOHP has very little effect on either the spectral parameters (Table I) or the general appearance of the spectrum. However, as the Cu:PPase ratio is raised first to 1.5 and then to 2.0 (parts c and d of Figure 2), the original hyperfine structure is retained, a new set of hyperfine structure in the $g_\parallel$ region (characterized by $g_\parallel$ and $A_\parallel$ values listed in Table I) and a broad shoulder at 322.5 mT become visible, and the spectral intensity of the $g_\perp$ peak continues to increase. Further increase in this ratio to 3.0, however, leads to both peak broadening and a loss of spectral intensity (Figure 2e), similar to that seen at a ratio of 2.0 in the absence of PCHOHP. In addition, the observed spectrum is no longer interpretable as the simple overlap of two different spectra. Because of the broadness of the peaks we have not attempted to resolve the observed spectrum into contributions from what is likely to be at least three different spectra. Therefore, no spectral parameters are listed in Table I for Figure 2e.

EPR spectra for a Cu(II)–PPase titration in the presence of Pi (Figure 3) show some differences when compared with the spectra already presented. Although they are broader (showing

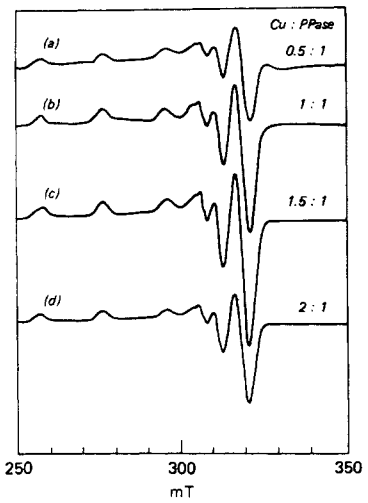

Figure 4. Frozen-state EPR spectra of solutions of PPase and varying Cu(II). Solutions had the following compositions: (a) 0.2 mM in PPase, 0.1 mM in Cu(II); (b) 0.2 mM Cu(II) and PPase; (c) 0.2 mM in PPase, 0.3 mM in Cu(II); (d) 0.2 mM in PPase, 0.4 mM in Cu(II). Temperature −94 °C. Receiver gain: (a–c) 1.6×10^3; (d) 1.2×10^3.

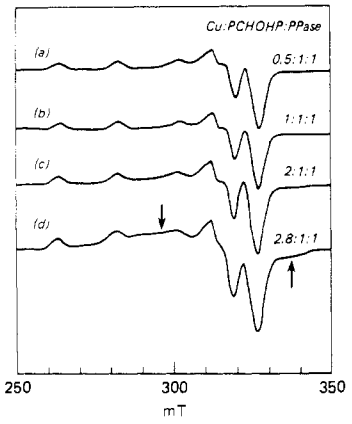

Figure 5. Frozen-state EPR spectra of solutions of PPase, PCHOHP, and varying Cu(II). All solutions were 0.2 mM in PPase subunits and PCHOHP and contained in addition (a) 0.2 mM Cu(II), (b) 0.3 mM Cu(II), (c) 0.4 mM Cu(II), or (d) 0.56 mM Cu(II). Arrows indicate the positions of the broad spectral features at 2925 and 3325 G. Temperature = −86 °C. Receiver gain for all spectra was 8×10^2.

no $A_\perp$ splitting) and less intense, the spectra at ratios of 0.5 and 1.0 (parts a and b of Figures 3) do allow evaluation of $g_\parallel$ and $A_\parallel$ (Table I). The values of these parameters, while quite different from those measured in the absence of phosphoryl ligand or in the presence of PCHOHP at corresponding Cu(II):PPase ratios, are in fact quite similar to those measured on addition of a second equivalent of Cu(II) in the presence of PCHOHP. Furthermore, addition of a second equivalent of Cu(II) to a solution of PPase and Pi leads to the just visible appearance of a second set of absorption lines (Figure 3c). The $g_\parallel$ and $A_\parallel$ values of these lines (Table I) correspond closely to those seen for the addition of the first Cu(II) to PPase in the presence or absence of PCHOHP. These results strongly suggest that the order of Cu(II) binding to various sites on PPase in the presence of Pi differs from that in the presence of PCHOHP.

Frozen-State EPR Spectra of Cu(II)–PPase in the Absence and Presence of Phosphoryl Ligands. Titrations similar to those presented above were also conducted on frozen solutions of Cu(II) and PPase, in part to increase the signal-to-noise ratio of the EPR spectra. The spectra obtained for all three sample series, Cu(II) and PPase alone (Figure 4) and Cu(II) and PPase in the presence of PCHOHP (Figure 5) or Pi (Figure 6), have similar g and A values for the main spectral features observed and share the additional property that in each case the spectral intensity of the main features, as measured by the $g_\perp$ line, does not markedly increase as the Cu(II):PPase ratio is increased beyond 1.0 (Table I). A unique aspect of the spectra of frozen solutions of Cu(II):PPase:PCHOHP is the appearance of broad spectral features, centered at approximately 292.5 and 332.5 mT, as the Cu(II):PPase ratio is raised beyond 2.0 (Figure 5d). The profound change in spectrum that accompanies an increase in Cu(II) stoichiometry beyond 2 equiv is clearly shown by comparison of the calculated difference spectrum obtained on subtraction of Figure 5b (Cu(II):PPase = 1.5) from Figure 5c (Cu(II):PPase = 2.0) with that obtained on subtraction of Figure 5c from Figure 5d (Cu(II):PPase = 2.8), as is done in Figure 7. Thus, whereas the former difference spectrum is very similar (albeit at lower intensity) to the observed spectrum in Figure 5a, the latter difference spectrum is totally different. It is broader, rather featureless, and not dissimilar from the spectra already described in Figures 1d and 2e.

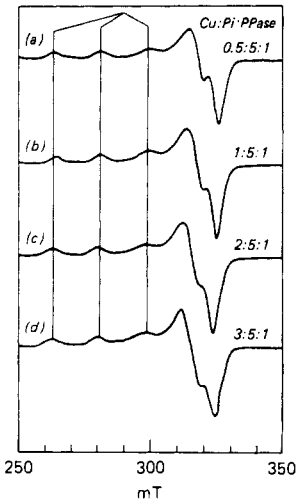

Figure 6. Frozen-state EPR spectra of solutions of PPase, Pi, and varying Cu(II). All solutions were 2.5 mM in PPase and 12.5 mM in Pi, and contained in addition (a) 1.25 mM Cu(II), (b) 2.5 mM Cu(II), (c) 5.0 mM Cu(II), (d) 7.5 mM Cu(II). Temperature = −35 °C. Receiver gain: (a–c) 4×10^2; (d) 3.2×10^2.

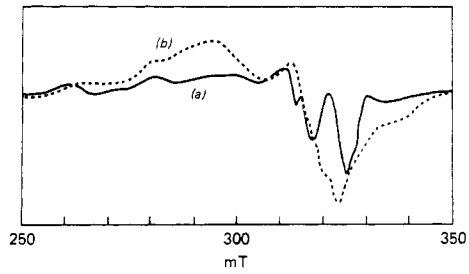

Figure 7. Difference spectra for frozen-state solutions of PPase, PCHOHP, and varying Cu(II): (a) Figure 5c, Cu:PPase 2:1, minus Figure 5b, Cu:PPase 1.5:1.0; (b) Figure 5d, Cu:PPase 3:1, minus Figure 5c.

It should be pointed out that no EPR signals were observed in the $g = 3$ or $g = 4$ regions for any of the solutions whose spectra are shown in Figures 1–6.

Effect of Mg^{2+} on the EPR Spectrum of a Cu(II)–PPase–PCHOHP Complex. The effect on the EPR spectrum of adding increasing amounts of Mg^{2+} to a solution of Cu(II)–PPase–PCHOHP (of composition 2.8:1.0:1.0) was examined in order to assess the competitiveness of Mg^{2+} for Cu(II) binding to PPase. As is clear from Figure 8, such addition leads to a disappearance of the broad spectral features at 292.5 and 332.5 mT, shown above to become prominent only when the number of Cu(II) equivalents is increased past 2 (Figure 5). In addition, the intensity of the spectrum is considerably increased (by about one-third). The EPR spectrum of a frozen solution having the composition Mg^{2+}:Cu(II):PPase:PCHOHP 100:2.8:1:1 (Figure 8c) is thus essentially identical with the EPR spectrum of a solution having a composition Cu(II):PPase:PCHOHP of 2.0:1.0:1.0 (as in Figure 5c). A plot of the intensity at 332.5 mT as a function of Mg^{2+} concentration (Figure 9) shows two clear inflections, the first at 0.5 mM and

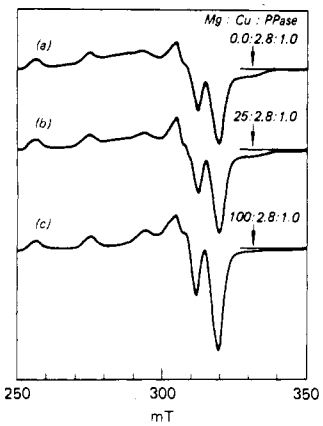

Figure 8. Effect of added Mg^{2+} on the frozen-state EPR spectra of the Cu(II)–PCHOHP–PPase complex. All solutions contained 0.2 mM PPase, 0.2 mM PCHOHP, and 0.56 mM Cu(II), with (a) no Mg^{2+}, (b) 4 mM Mg^{2+}, or (c) 20 mM Mg^{2+}. Temperature = −87 °C. During titration, all spectral parameters were kept the same. Note the decrease in intensity of the shoulder at 3325 G (↓) as the Mg^{2+} concentration is raised.

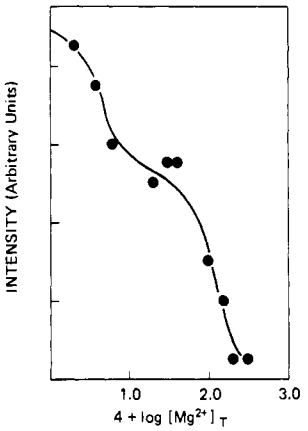

Figure 9. Titration plot showing the decrease in intensity of the shoulder at 3325 G as a function of added Mg^{2+} to a frozen solution containing 0.2 mM PPase, 0.2 mM PCHOHP, and 0.56 mM Cu(II). Temperature = −87 °C.

the second at 12 mM. Further addition of Mg^{2+} up to a total Mg^{2+} concentration of 150 mM gave an EPR spectrum essentially unchanged from that seen in Figure 8c.

It should be noted that this study was carried out in the frozen state rather than the liquid state in order to take advantage of the higher intensity for Cu(II) EPR detection obtainable at lower temperatures. Such higher intensity allows spectra to be taken at lower concentrations of Cu(II) and PPase [2.7 mM PPase at −6 °C (Figure 2) vs. 0.2 mM PPase at −87 °C (Figure 5)], in turn permitting the achievement of high molar ratios of Mg^{2+} over Cu(II) at reasonable Mg^{2+} concentrations.

Spin-Echo Studies of Cu(II)–PPase in the Absence and Presence of PCHOHP. Spin-echo measurements of T_1 were made at 10 K on frozen solutions of Cu(II) and PPase (±PCHOHP) paralleling those described above. Sample data are shown in Figure 10, and the collected T_1 measurements are displayed in Table II. As may be seen, the value of T_1 at a Cu(II):PPase ratio of 1.0, in the presence or absence of PCHOHP, is similar to that for the magnetically isolated Cu(II) in Cu(II) hexafluoroacetylacetonate. In the absence of PCHOHP, raising the ratio to 2.0 results in a more than twofold decrease in T_1. No further decrease is seen when the ratio is raised further to 3.0. In the presence of PCHOHP, by contrast, there is a progressive decrease in T_1 as the Cu(II):PPase ratio is raised from 1.0 to 2.0 and 3.0, to a value experimentally indistinguishable from that measured in the absence of PCHOHP, and no further decrease at a ratio of 4.0.

ESEEM Measurements. The method of electron spin echo envelope modulation (ESEEM) was employed in an attempt to identify ligands bound to the copper atoms.[22] This method is based upon the possible modulation, by a neighboring nucleus of nonzero spin, of the decay of the spin echo amplitude as a function of pulse separation, when an appropriate pulse sequence is used. The period of the modulation is dependent upon the strength of the coupling between the nucleus and the electron that gives rise

Table II. Spin–Lattice Relaxation Times, T_1[a]

Cu atoms per subunit	T_1, μs	
	with PCHOHP	without PCHOHP
1	150 ± 16	174 ± 21
2	117 ± 15	75 ± 10
3	67 ± 10	75 ± 14
4	85 ± 21	

[a] Spin–lattice relaxation times (T_1) of unpaired electrons in copper complexes of PPase, at 10 K, for $g = 2.06$. For $[CuF_6AcAc]$ $T_1 = 214 \pm 10$ ($^+F_6AcAc$ is hexafluoroacetylacetonate).

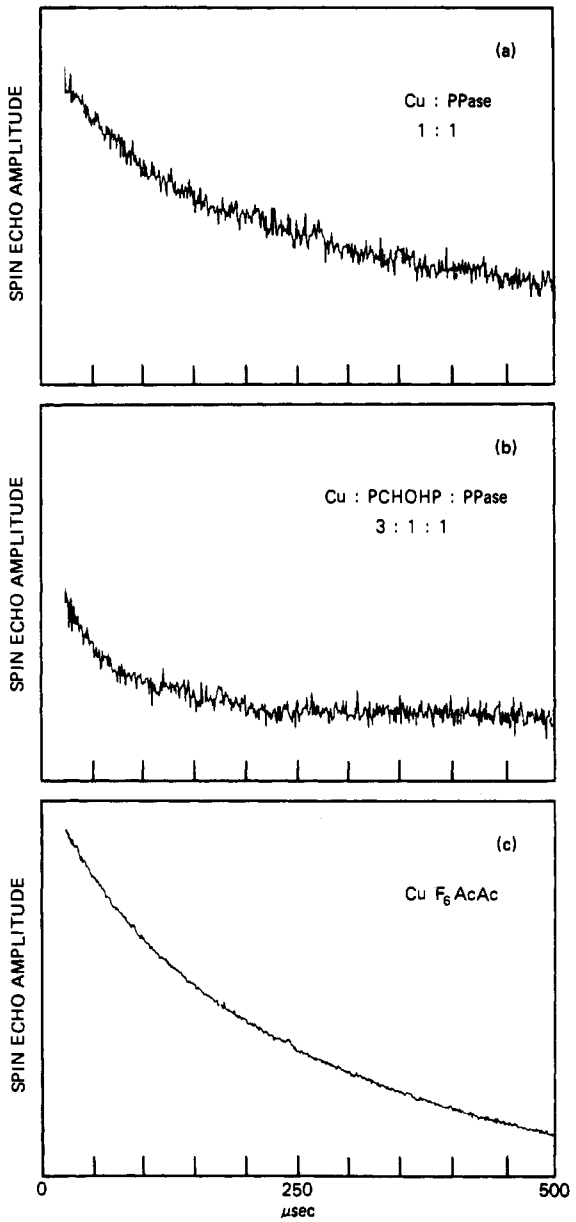

Figure 10. Traces of three-pulse echo amplitudes as a function of time: (a) 1 mM in PPase and Cu(II); (b) 1 mM in PPase and PCHOHP and 3 mM in Cu(II); (c) 3 mM in copper hexafluoroacetylacetonate. Temperature = 10 K.

(22) Thomann, H.; Dalton, L. R.; Dalton, L. A. *Biol. Magn. Reson.* **1984**, *6*, 143.

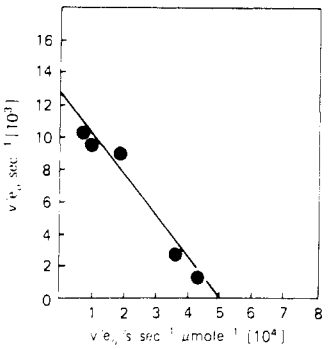

Figure 11. Eadie–Hofstee plot of PPase-catalyzed hydrolysis of PPi. Temperature = 27 °C; pH = 7.2. [Cu(II)] = 0.4 mM; [PPi] = 7.5–100 μM. In the absence of Cu(II), no measurable rate of PPi hydrolysis was observed.

Table III. Activity Study of Cu(II)–PPase

metal ion	pH	k_{cat}(hyd), s^{-1}	K_M(hyd), μM
Mg^{2+}	7.0	212[a]	4.3[a]
Mn(II)	7.0	22[a]	20[a]
Cu(II)	7.2	0.16	26.5
none	7.2	<0.001	

[a] Values from ref 22.

to the spin echo. The modulated echo envelope is analyzed primarily by computing its Fourier transform to determine the component frequencies. ESEEM measurements on Cu(II)–PPase solutions were made in the presence and absence of PCHOHP, as well as in the presence of ^{17}O-labeled PCHOHP. In no case was any evidence obtained for nuclear (either ^{14}N or ^{17}O) modulation of the electron spin echo.

Cu(II)–PPase Catalysis of Pyrophosphate Hydrolysis. Eadie–Hofstee plots of steady-state rate constants for PPase-catalyzed PPi hydrolysis in presence of Cu(II) at pH 7.2 are shown in Figure 11. The derived values of k_{cat} and K_M are presented in Table III along with previously determined values measured in the presence of Mg^{2+} and Mn(II).[23]

Discussion

Cu(II) Sites: Structures, Relative Affinities, and Mutual Interactions. Our study of the EPR spectra and T_1 values of Cu(II) complexes of PPase provides useful information about both the structure of the Cu(II) binding sites and the interaction between enzyme-bound Cu(II) sites. Specifically, our results are consistent with a three-site model for Cu(II) binding to PPase (Figure 12A) having the following characteristics:

(i) Binding to two of the sites (A and B) takes place in the absence of added phosphoryl ligand.

(ii) Site A is filled first and appears to contain only oxygen ligands to Cu(II).

(iii) Cu(II) bound to sites A and B show strong spin–spin interaction.

(iv) Binding to site C is dependent on the presence of a phosphoryl ligand.

(v) The order in which sites A, B, and C are filled depends upon the nature of the phosphoryl ligand. The order is A, C, B in the presence of PCHOHP and C, A, B in the presence of Pi.

(vi) Cu(II) in site C interacts more weakly with Cu(II) in site A than does Cu(II) in site B. The site (B)–site (C) interaction is intermediate between the A–B and A–C interactions.

(vii) Mg^{2+} competes strongly with Cu(II) for binding to at least one site, most likely site B.

The following discussion deals with our results in terms of this model.

EPR spectra of liquid solutions containing up to 1 equiv of Cu(II) bound per PPase in the absence of phosphoryl ligand (Figure 1 and Table I) are characterized by a relatively high value

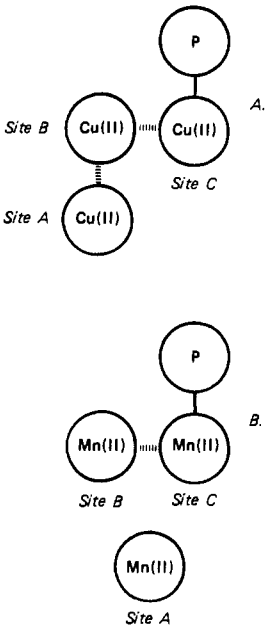

Figure 12. Models for (A) Cu(II) and (B) Mn(II)[10] binding to PPase. Dashed lines indicate strong dipole–dipole interactions. P refers to an active-site-bound phosphoryl ligand.

of $g_\parallel$ (2.38), a rather small value of $A_\parallel$ (144 × 10^{-4} cm^{-1}), and narrow hyperfine lines (line width = 1.5 mT), features that have previously been interpreted as indicating exclusive oxygen coordination to Cu(II) in a distorted octahedral complex.[24] This result is consistent with earlier results showing that other divalent metal ions, such as Cd^{2+} and Co(II), bind to PPase with exclusive oxygen ligand coordination.[7] Addition of a second Cu(II) results in line broadening and loss of spectral intensity, indicative of a strong Cu(II)–Cu(II) spin–spin interaction. The loss of intensity and the broadening are not results of superposition of spectra from two noninteracting Cu(II) ions, as indicated by the approximately twofold reduction in the observed value of T_1 that accompanies addition of a second Cu(II) (Table II). The lack of effect of the third equivalent of Cu(II) demonstrates that the effect of the second Cu(II) is not due to free Cu(II) in solution. It is noteworthy that spectral intensity increases linearly with added Cu(II) up to 1 equiv and then decreases slightly, a clear indication that the affinity for site A is significantly greater than that for site B. This interpretation is in accord with evidence, previously obtained by Höhne and Heitmann[25] by fluorescence quenching experiments, that, in the absence of phosphoryl ligands, PPase has a unique site of high affinity for Cu(II) [K_d = 0.1–1.0 μM] as well as a site of lower Cu(II) affinity.

Some limits may be placed on the distance between sites A and B. The absence of a $\Delta M = 2$ transition implies a lower limit of no less than 5–6 Å,[26] while the pronounced effects seen on line width, spectral intensity, and T_1 suggest an upper limit of no more than 8–10 Å.[27]

The most straightforward interpretation of the EPR spectra obtained on Cu(II) titration of PPase in the presence of PCHOHP in liquid solution (Figure 2) and of the T_1 data in Table II is that site A is filled first, that the second equivalent of Cu(II) goes primarily to site C, whle the third equivalent goes primarily to site B. Thus, for solutions with a Cu(II):PPase ratio of 1.0, the EPR spectrum is the same in both the absence and the presence of PCHOHP (Figures 1b and 2b) and, as discussed above, reflects Cu(II) binding to site A. At a ratio of 1.5, however, the presence of PCHOHP results in the appearance of a second hyperfine splitting pattern that is superimposed on that due to site A binding

(23) Welsh, K. M.; Jacobyansky, A.; Springs, B.; Cooperman, B. S. *Biochemistry* **1983**, *22*, 2243.
(24) Branden, R.; Nilsson, T.; Styring, S. *Biochemistry* **1984**, *23*, 4373.
(25) Höhne, W. E.; Heitmann, P. *Acta. Biol. Med. Ger.* **1978**, *37*, 375.
(26) Solomon, E. I. *Pure Appl. Chem.* **1983**, *55*, 1069.
(27) Eaton, S. S.; DuBois, D. L.; Boymel, P. M.; Eaton, G. R. *J. Phys. Chem.* **1979**, *83*, 3323.

(Figure 2c). As compared with site A binding, this latter pattern is characterized by a lower value of g (2.27), a higher value of $A_{\parallel}$ (175×10^{-4} cm^{-1}) and broader hyperfine lines (line width ranging from 3 to 4.5 mT), and we attribute it to the binding of Cu(II) to site C. Raising the Cu(II):PPase ratio to 2.0 leads to very little broadening of either pattern (Figure 2d), but at a ratio of 3.0 both patterns are broadened. This suggests that the strong site A–site B interaction is maintained in the presence of PCHOHP, and that there is also an interaction between the Cu(II) ions bound in sites B and C. The variation in T_1 as a function of the Cu(II):PPase ratio (Table II) is at least partially consistent with interpretation, since the maximum decrease is not seen until the ratio reaches 3. It is true that there is a progressive decrease in T_1 accompanying the addition of first a second and then a third Cu(II) per PPase subunit, whereas according to our model of weak site A–site C interaction one might have expected little change in T_1 following addition of a second Cu(II). The observed change probably reflects the greater sensitivity of T_1 measurement as compared with apparent line width measurement in a complex spectrum (Figure 2c,d). In addition, the angular dependence of the dipolar relaxation process might favor relaxation from the A–C interaction more than from the B–C interaction for the particular g value at which T_1 was measured. A third possibility is that the relative affinity of Cu(II) for sites B and C is temperature-dependent and that a greater fraction of the second added Cu(II) is bound in site B at the lower temperature used in T_1 measurement (10 K) than at the higher temperature used in taking liquid-state EPR spectra (267 K).

The most obvious difference in the liquid-state EPR spectra obtained in the presence of Pi as compared to those obtained in either the presence of PCHOHP or the absence of any phosphoryl ligand is that the first Cu(II) added has an EPR spectrum essentially identical with that we have assigned to site C rather than to site A (Figure 3a,b). This result suggests that, in the presence of Pi, the order in which sites are filled is C, A, B, which contrasts with the order A, C, B in the presence of PCHOHP.

It is important to note that the use of the 180°–90°–180° pulse sequence may produce values of T_1 that are artificially shortened somewhat by spectral diffusion effects.[22] However, since the object of the pulsed EPR measurements is to detect changes in T_1 as a function of the copper:subunit ratio, the conclusion drawn from these results would not be altered by the presence of spectral diffusion.

EPR spectra of frozen solutions of Cu(II)–PPase in the presence or absence of PCHOHP or Pi are considerably less informative than those obtained in liquid solution, presumably because the much broader $g_{\parallel}$ lines obtained for frozen solutions (~4 mT measured as width at half-height) as compared to their liquid-state counterparts (~1.5 mT) masks any dipolar line broadening resulting from site–site interaction. In the absence of phosphoryl ligand (Figure 4) each spectrum obtained over a Cu(II):PPase range of 0.5–2.0 appears to reflect binding to a single site or to more than one similar but noninteracting site and there is a clear difference in the spectral parameters for this site or sites compared to what is seen in liquid solution for site A (Table I). Spectral parameters for some well-defined Cu(II) complexes have been shown to be temperature-dependent, presumably reflecting changes or distortions in Cu(II) coordination stereochemistry,[28] and it is possible a similar effect is important for site A. Alternatively, it may be that there is an actual change in ligand field at site A as the temperature is lowered. The parameters measured in frozen solution would certainly be consistent with replacement by one or more nitrogen of the oxygens coordinated to Cu(II) in site A in liquid solution.[12] Such a temperature-dependent replacement would also be consistent with the expected increase in the ratio of Lewis basicities of nitrogen to oxygen as the temperature is decreased.[29]

The absence of an ESEEM effect does not rule out direct liganding of Cu(II) by ^{14}N, since the superhyperfine couplings produced by such a configuration generally are too large to be measured by the ESEEM method. However, it does provide strong evidence against an imidazole ligand, since the remote (nonligand) nitrogen of the imidazole should give rise to intense modulation of the Cu(II) spin echo.[30] Here it is interesting to note the complete absence of histidine side chains in the active site tentatively identified by the X-ray crystallographic studies of PPase.[31,32]

By contrast, no conclusion can be drawn from the absence of ^{17}O modulations, for two reasons. Modulations from ^{17}O have rarely, if ever, been observed in any system, possibly because the high nuclear spin ($^5/_2$), combined with nuclear quadrupole splittings, causes severe broadening and overlap of frequency components. This is a particularly serious problem in nonoriented systems. Also, a directly coupled ^{17}O may also be too strongly coupled to be observed, even under ideal conditions. Thus, this result is reported merely as an observation.

Relationship of Cu(II) Binding to PPase to the Binding of Other Divalent Metal Ions. Although Cu(II) binding to PPase is strongly influenced by phosphoryl ligands known to bind to the active site of PPase and added Cu(II) not only acts as a cofactor for PPase but also inhibits the higher activity found in the presence of Mg^{2+},[33] the very low activity conferred by Cu(II) does raise the question as to how closely related the Cu(II) sites we monitor by EPR are to the binding sites for divalent metal ions confering higher activity, such as Mg^{2+} or Mn^{2+}. The results described in Figures 8 and 9 demonstrate strong competition by Mg^{2+} for the site bound by the last added Cu(II) in a frozen solution of composition Cu(II):PPase:PCHOHP = 2.8:1.0:1.0. That the spectrum due to this site (Figure 7) has very broad features suggests that it is a site having a strong spin–spin interaction with one or both of the other Cu(II) sites. On the basis of our previous discussion, a likely candidate is site B.

Two inflection points are observed in the Mg^{2+} titration curve (Figure 9). Given that (a) the results in Figure 7 suggest that Mg^{2+} displaces a single Cu(II), (b) the spectral change associated with the second inflection point is greater than that associated with the first, (c) Cu(II) affinities for bi- and tridentate oxygen ligands are 10^4 to 10^7 times greater than the corresponding Mg^{2+} affinities[34] (the ratios for nitrogen containing ligands are still larger[34]), and (d) the first inflection point occurs at a ratio of total Cu(II) concentration to total Mg^{2+} concentration of about 1.0, the most plausible interpretation of the titration curve is that the first inflection reflects an allosteric effect of direct Mg^{2+} binding to a site not occupied by Cu(II) whereas the second inflection results from a direct competition by Mg^{2+} for a Cu(II) binding site. From the ratios of the affinities of model complexes of Cu(II) and Mg^{2+}, this site must be quite specific for Mg^{2+}, since the second inflection point occurs at an effective ratio of Mg^{2+}:Cu(II) of only 60 or so. At higher ratios, Mg^{2+} might well compete for the tighter binding sites seen by Cu(II) EPR (Figure 8). For example, Höhne and Heitmann[25] have shown that Mg^{2+} does not displace tightly bound Cu(II) at a Mg^{2+}:Cu(II) ratio of 300, but that it does displace such Cu(II) at a ratio of 8000.

It is also of interest to compare the relative orientation of the three Cu(II) sites (Figure 12A) with the relative orientations of enzyme-bound divalent metal ions found in previous studies.[8,10] Using Mn(II) EPR as a probe, we[10] found that (1) titration of PPase with Mn(II) in the absence of a phosphoryl ligand shows evidence for only a weak Mn(II)–Mn(II) interaction, with an estimated Mn(II)–Mn(II) distance of >10 Å, (2) titration of

(28) Boas, J. F.; Pilbrow, J. R.; Hartzell, C. R.; Smith, T. D. *J. Chem. Soc. A* **1969**, 572.
(29) Bell, R. P. *The Proton in Chemistry*; Cornell University: Ithaca, New York, 1959; p 62.
(30) Mims, W. B.; Peisach, J. J. *Chem. Phys.* **1978**, *69* (II), 4921.
(31) Kuranova, I. P.; Terzyan, S. S.; Voronova, A. A.; Smirnova, E. A.; Vainstein, B. K.; Höhne, W.; Hansen, G. *Bioorg. Khim.* **1983**, *9*, 1611.
(32) Terzyan, S. S.; Voronova, A. A.; Smirnova, E. A.; Kuranova, I. P.; Nekrasov, Yu. V.; Harutyunyan, E. G.; Vainstein, B. K.; Höhne, W.; Hansen, G. *Bioorg. Khim.* **1984**, *10*, 1469.
(33) Moe, O. A.; Pham, S.; Selinsky, B.; Dang, T. *Biochim. Biophys. Acta* **1985**, *827*, 207.
(34) Hanzlik, Robert P. *Inorganic Aspects of Biological and Organic Chemistry*; Academic: New York, 1972; p 127.

PPase with Mn(II) in the presence of PCHOHP gives evidence for a strong Mn(II)-Mn(II) interaction with an estimated distance of <7-8 Å, and (3) titration of a PPase-Mn(II)-PCHOHP complex with Ca^{2+} leads to the binding of 1.0 Ca^{2+} per PPase subunit with a loss of the strong Mn(II)-Mn(II) interaction. These observations, taken together with earlier results showing that (a) CaPPi, but not free Ca^{2+}, binds tightly to PPase[35] and (b) PPase binds two Mn(II) ions per subunit in the absence of phosphoryl ligand and three to four Mn(II) ions in the presence of phosphoryl ligand (see above), led us to propose the schematic model for Mn(II) binding to PPase shown in Figure 12B. Here, two Mn(II) ions bind to sites A and B in the absence of phosphoryl ligand and these sites interact only weakly, whereas site C, to which Mn(II) binds in the presence of phosphoryl ligand, has a strong interaction with site A and/or B. According to this model, added Ca^{2+} in the presence of PCHOHP binds uniquely to site C, thus eliminating the strong Mn(II)-Mn(II) interaction.

Subsequently, Knight et al.[8] reported results generally consistent with the model shown in Figure 12B. They studied the effect of Cr(III) and Co(III) complexes of Pi and imidodiphosphate (PNP) on the EPR of enzyme-bound Mn(II) and on the proton relaxation rate of H_2O bound to enzyme-Mn(II). In this work, these authors reported a weak Mn(II)-Mn(II) interaction in the absence of an added phosphoryl ligand (estimated distance 11-14 Å), corresponding to occupancy of sites A and B, a strong Mn(II)-Cr(III) interaction (estimated distances 4.8-5.2 Å for the Pi complex and 7.0-7.5 Å for PNP complexes), corresponding to the site B-site C interaction, and a weaker Mn(II)-Mn(II) interaction in the presence of Co(III) complexes (estimated distance 7-8 Å for the Pi complex and 8-10 Å for the PNP complex), which would indicate that sites A and B are closer together in the presence of a metal ion-phosphoryl ligand complex than in its absence.

The major difference between Cu(II) and Mn(II) binding to PPase, as reflected in Figure 12, is that the two Cu(II) ions bound in the absence of phosphoryl ligand interact with each other more strongly than either does with the Cu(II) bound in the presence of either PCHOHP or of Pi (Figure 12A). These differences between Cu(II) binding and Mn(II) binding may reflect subtle differences in coordination geometry and/or in ligand identity at what are basically the same or largely overlapping sites. Such sites presumably fall within the large active-site cleft found by X-ray crystallographic structural analysis of PPase, which contains at least four divalent metal ion binding sites.[32,33] Alternatively, it is possible that at least some Cu(II) binding to PPase takes place at sites quite distinct from those sites occupied by Mn(II). Our previous studies of Cd^{2+} binding to PPase[7,9] may be relevant in this regard. Cd^{2+}, like Cu(II), confers only very low enzyme activity on PPase. Of the four Cd^{2+} sites per PPase subunit that we observe both by direct binding studies and by ^{113}Cd NMR studies, only two are directly competed for by Mg^{2+}. The other two are believed to bind at sites distinct from the active site. Clearly, additional experiments will be needed in order to distinguish between these two possibilities.

Acknowledgment. We wish to thank Dr. G.H. Reed for sharing his knowledge of EPR with us and Dr. T. Ohnishi for the use of an X-band EPR instrument. This work was supported by NIH Grants AM-13212 to B.S.C. and GM-25052 to J. S. Leigh in the Biochemistry and Biophysics Department.

Registry No. PPase, 9024-82-2; $PCHOHPO_4$, 15468-10-7; Cu, 7440-50-8; PO_4^{3-}, 14265-44-2.

(35) Ridlington, J. W.; Butler, L. G. *J. Biol. Chem.* **1972**, *247*, 7303.

Contribution from the Department of Chemistry, North Carolina State University, Raleigh, North Carolina 27695-8204, and AT&T Bell Laboratories, Murray Hill, New Jersey 07974

Band Electronic Structure of the Molybdenum Blue Bronze $A_{0.30}MoO_3$ (A = K, Rb)

M.-H. Whangbo*[†1a] and L. F. Schneemeyer*[1b]

Received June 7, 1985

The electronic structure of the blue bronze $A_{0.30}MoO_3$ (A = K, Rb) was examined by performing tight-binding band calculations on a number of model chains and an $Mo_{10}O_{30}$ slab. When normalized to $A_3Mo_{10}O_{30}$ (i.e., half the unit cell), the bottom two d-block bands of an $Mo_{10}O_{30}$ slab are partially filled. The Fermi surfaces of these two bands are open along the interchain direction, in agreement with the experimental fact that the blue bronze is a pseudo-one-dimensional metal with good electrical conductivity along the chain direction *b*. The Fermi surfaces of the two bands are curved due to interactions between adjacent $Mo_{10}O_{32}$ chains, but the curvatures of the Fermi surfaces are opposite for the two bands. Thus the two pieces of the first-band Fermi surface are nested to those of the second-band Fermi surface by a single wave vector $q_b \simeq 0.75b^*$, which explains why only one charge density wave occurs in the blue bronze. For an $Mo_{10}O_{30}$ slab, the bottom of the third d-block band is calculated to lie above, but very close to, the Fermi level (i.e., 0.012 eV above e_f). This feature is responsible for the temperature dependence of q_b in the blue bronze, which increases gradually from $\sim 0.72b^*$ at room temperature to $\sim 0.75b^*$ below the metal-to-semiconductor phase-transition temperature.

Solid oxide phases with a range of composition $A_xM_yO_z$ (A = alkali metal, M = transition metal) are generally referred to as bronzes,[2] since they exhibit intense color and metallic luster in most cases. In the $A_xM_yO_z$ bronze, an alkali metal donates its valence electron to the d-block bands of the transition metal. Thus, whether the bronze is a metal or a semiconductor depends upon the nature of its d-block bands. So far three well-defined molybdenum bronzes $A_{0.33}MoO_3$ (A = K), $A_{0.30}MoO_3$ (A = K, Rb) and $A_{0.9}Mo_6O_{17}$ (A = Li, Na, K), have been synthesized and studied. The red bronze[3,4] $A_{0.33}MoO_3$ is a semiconductor at all temperatures,[5] while the purple bronze[3,6] $A_{0.9}Mo_6O_{17}$ is a quasi-two-dimensional (2D) metal.[7]

The blue bronze[3,8] $A_{0.30}MoO_3$ exhibits a metal-to-semiconductor transition at T_c = 180 K,[9] and its electrical properties are strongly anisotropic.[10] On the basis of optical reflectivity data, Travaglini et al.[11] suggested that the blue bronze is a quasi-one-dimensional

[†] Camille and Henry Dreyfus Teacher-Scholar (1980-1985).

(1) (a) North Carolina State University. (b) AT&T Bell Laboratories.
(2) (a) Sienko, M. J. *Nonstoichiometric Compounds*; Gould, R. F., Ed.; American Chemical Society: Washington, DC, 1963; p 224. (b) Hagenmuller, P. *Prog. Solid State Chem.* **1971**, *5*, 71. (c) Wells, A. F. *Structural Inorganic Chemistry*, 5th ed.; Clarendon: Oxford, 1984; p 612. (d) Schlenker, C.; Dumas, J.; Escribe-Filippini, C.; Guyot, H.; Marcus, J.; Fourcaudot, G. *Philos. Mag. B* **1985**, *52*, 643.
(3) Wold, A.; Kunnmann, W.; Arnott, R. J.; Ferretti, A. *Inorg. Chem.* **1964**, *3*, 345.
(4) Stephenson, N. C.; Wadsley, A. D. *Acta Crystallogr.* **1965**, *18*, 241.
(5) Bouchard, G. H.; Perlstein, J. H.; Sienko, M. J. *Inorg. Chem.* **1967**, *6*, 1682.
(6) (a) Stephenson, N. C. *Acta Crystallogr.* **1966**, *20*, 59. (b) Reau, J. M.; Fouassier, C.; Hagenmuller, P. *J. Solid State Chem.* **1970**, *1*, 326. (c) Gatehouse, B. M.; Lloyd, D. J.; Miskin, B. K. *NBS Spec. Publ. (U.S.)* **1972**, *No. 364*, 15. (d) Vincent, H.; Ghedira, M.; Marcus, J.; Mercier, J.; Schlenker, C. *J. Solid State Chem.* **1983**, *47*, 112.

0020-1669/86/1325-2424$01.50/0